REPORT DOCUMENTATION PAGE

Form Approved
OMB No. 0704-0188

1. REPORT DATE	2. REPORT TYPE	3. DATES COVERED
	Professional Paper	

4. TITLE AND SUBTITLE	5a. CONTRACT NUMBER
Thermography for the Characterization of Corrosion Damage	5b. GRANT NUMBER
	5c. PROGRAM ELEMENT NUMBER

6. AUTHOR(S)	5d. PROJECT NUMBER
Ignacio Perez Paul Kulowitch	5e. TASK NUMBER
	5f. WORK UNIT NUMBER

7. PERFORMING ORGANIZATION NAME(S) AND ADDRESS(ES)	8. PERFORMING ORGANIZATION REPORT NUMBER
Naval Air Warfare Center Aircraft Division 22347 Cedar Point Road, Unit #6 Patuxent River, Maryland 20670-1161	

9. SPONSORING/MONITORING AGENCY NAME(S) AND ADDRESS(ES)	10. SPONSOR/MONITOR'S ACRONYM(S)
Naval Air Systems Command 47123 Buse Road Unit IPT Patuxent River, Maryland 20670-1547	11. SPONSOR/MONITOR'S REPORT NUMBER(S)

12. DISTRIBUTION/AVAILABILITY STATEMENT

Approved for public release; distribution is unlimited.

13. SUPPLEMENTARY NOTES

14. ABSTRACT

Thermography is a viable NDE technique for the characterization of corrosion in metallic materials. Thermography is a rapid, non-contact, wide area inspection technique that is easy to interpret and that is not significantly sensitive to material curvature. We have developed a portable system and have characterized the sensitivity of the technique. Results will be presented in this paper.

15. SUBJECT TERMS

Thermography; thermographic inspection; corrosion; naval aviation; corrosive environment; lateral heat effects

16. SECURITY CLASSIFICATION OF:			17. LIMITATION OF ABSTRACT	18. NUMBER OF PAGES	19a. NAME OF RESPONSIBLE PERSON
a. REPORT	b. ABSTRACT	c. THIS PAGE			19b. TELEPHONE NUMBER (include area code)
Unclassified	Unclassified	Unclassified	Unclassified	8	Ignacio Perez (301) 342-8074

Thermography for Characterization of Corrosion Damage

Ignacio Perez and Paul Kulowitch
Naval Air Warfare Center, Aircraft Division
Patuxent River MD 20670

ABSTRACT

Thermography is a viable NDE technique for the characterization of corrosion in metallic materials. Thermography is a rapid, non-contact, wide area inspection technique that is easy to interpret and that in not significantly sensitive to material curvature. We have developed a portable system and have characterized the sensitivity of the technique. Results will be presented in this paper.

Keywords: Thermography, thermographic inspection, corrosion, naval aviation, corrosive environment, lateral heat effects.

INTRODUCTION

The Navy operates in the most corrosive environment of any of the DoD services or commercial aviation. As a result corrosion prevention, detection and repair are of outmost importance to the Navy. All the materials in our platform are designed and engineered to offer the maximum corrosion protection without limiting their structural characteristics. New paint system are being develop that comply with EPA regulations while providing enhanced protection against the environment. No matter how much protection we provide to our platforms in the form of improved materials, sealants and paints, the environment ultimately will penetrate the coating and initiate corrosion. This process can be exacerbated or mitigated by the specific mission of the platform. Low flying antisubmarine aircraft will corrode at an accelerated rate when compared to high altitude flying communication aircraft.

The cost of corrosion control is enormous and accelerating as our fleet ages. This is especially significant in today's environment of reduced budgets and decreasing personnel. With fewer new acquisition, the Navy is increasingly being forced to extend the life of existing platforms beyond their original design life to meet mission requirements. In order to maintain fleet readiness and safety improved inspection methods are required that can detect the occurrence of corrosion fast and reliably.

New techniques are being developed at the Naval Air Warfare Center aimed at the reliable and rapid inspection of corrosion in Naval aircraft. One of such techniques is pulsed thermography. This is a wide area inspection technique which is especially suited for the detection of hidden corrosion. It requires no contact media to perform the inspection as opposed to more conventional techniques such as ultrasonic inspection. This technique relies on the thermal gradients that result from the interaction between the

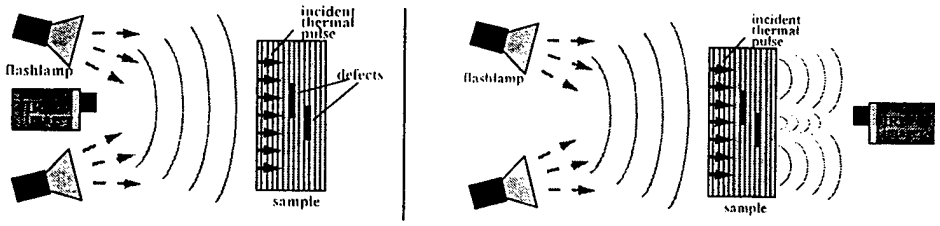

Fig. 1. (Left) Shows a standard single side inspection setup with the IR camera and the arc lamps in the same side. (Right) Shows a through transmission setup which in general provides twice the depth of resolution.

thermal fields and defects present in the structure. This technique is also significantly insensitive to curvature and is relative easy of interpretation.

EXPERIMENTAL

The minimum number of experimental components needed to perform pulsed thermography are a heat source and an infrared (IR) camera. The proper choice of heat source is paramount for a successful thermographic experiment. Such source must be chosen so as to maximize the thermal contrast between the defect and the surrounding material. In some cases one can maximize the thermal contrast by heating the defect exclusively without disrupting the surrounding material such as when using microwave energy for detecting water entrapped inside a ceramic material. The microwave energy will propagate through the ceramic material without heating it and finally will be absorbed by any water present in it. The previous approach is not always possible and one has to resort to exploiting other defect features (such as geometrical features) to enhance the thermal contrast. The most common energy sources used to thermally excite materials are: air heat guns, microwave sources, infrared lamps and arc lamps. All the samples studied in this paper were thermally excited using a pair of xenon arc lamps, each one powered by a 5 KJoule capacitor bank with a 10 msec discharge time. The IR camera used in these experiments was a Amber Engineering InSb focal plane array (128 x 128) camera with silicon optics operating in the 3 - 5 micron spectral range. Figure 1 left (single side inspection setup) shows the experimental configuration used to image all defects. Other experimental arrangements are possible such as the one shown on Fig. 1 right (through transmission setup). This setup is not well suited for field inspections where only one side is typically exposed, but has twice the depth of resolution than single side inspection methods. Figure 2 shows the camera system and arc lamps used to acquire data for this paper.

Fig. 2: Thermal imaging system used to acquire data.

Any material can be inspected thermographically (such as metals, ceramics and composites) but the outcome of the inspection will depend on many factors such as sample geometry, sample thickness, amount of heat used, surface emissivity, specific heat, material density, thermal

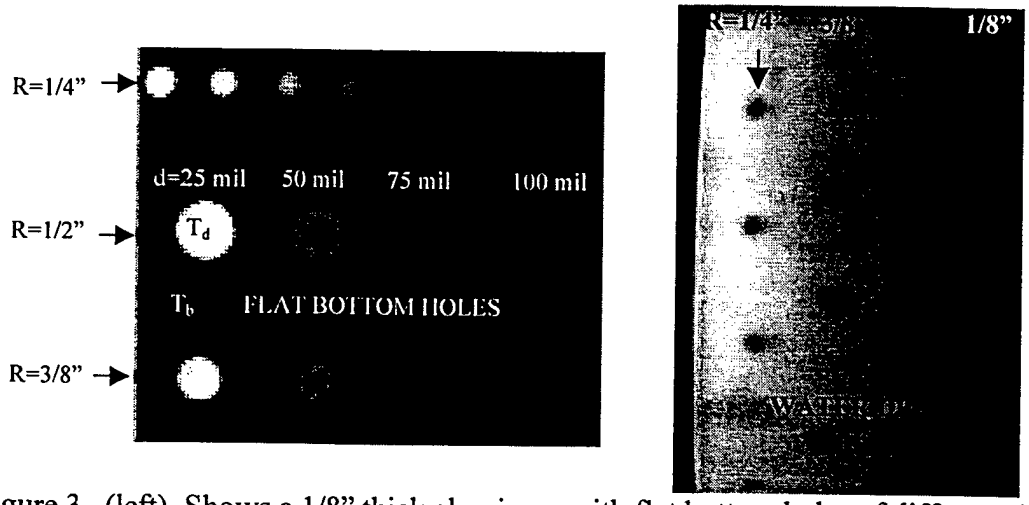

Figure 3. (left) Shows a 1/8" thick aluminum with flat bottom holes of different depth ranging from 25 mil to 100 mil and three different radii of R=1/2",3/8" and 1/4". (Right) Shows a 1/32" thick aluminum panel with water drops of different radii and different water content.

conductivity, defect depth and the size of the defect and other parameters. To gain insight into the effect that several of these parameters have on the thermographic process we fabricated various aluminum 7075T6 panels with embedded defects. One panel was fabricated with flat bottom holes while the others had water pockets on the back. Figure 3 shows two thermal images a few msec after exposure to a heat pulse. The figure on the left corresponds to a t_o=1/8" thick aluminum panel with three different radii flat bottom holes (R=1/2", 3/8" and 1/4" diameter). Flat bottom holes are a crude simulation to material loss that results from the corrosion process, but offer a simple means of generating standards for the characterization of the thermal process. The distance from the surface of the panel to the surface of the flat bottom holes (also referred as the defect depth "d") ranged from 25 mil to 100 mil. The largest contrast corresponds to the defect closest to the surface while the defect furthest from the surface showed the smallest thermal contrast. The thermal contrast is defined as the difference of the temperature above the defect (T_d on fig 3) from the temperature of a point away from the defect area (such as T_b on fig. 3). The center to center distance between flat bottom holes was set to at least 2 diameters to minimize inter-hole proximity effects.

Water entrapment is a leading cause of corrosion and debonding in honeycomb structures. Early detection of it leads to economical repairs. Figure 3 right shows the thermal image a few msec after exposure of one of three panels (panel thickness were t_o=1/32", 1/16" and 1/8") fabricated to model water entrapment. The panel shown on that figure corresponds to a t_o=1/32" thick aluminum panel with water drops on the back of different diameters (1/8", 1/4", 3/8"and 1/2" diameter) and with different amount of water in them. Water was contained on the back of the panels by gluing straws of different diameters to the surface and by filling them with water up to different levels. The heights of water used were d = 1/16", 1/8", 3/16" and 1/4". It is clear from Fig. 3 right that the amount of water has little effect on the thermal contrast (notice the small contrast variation among drops of equal radii). The straws were staggered to maximize the spacing among them in order to minimize proximity effects. It is interesting to note

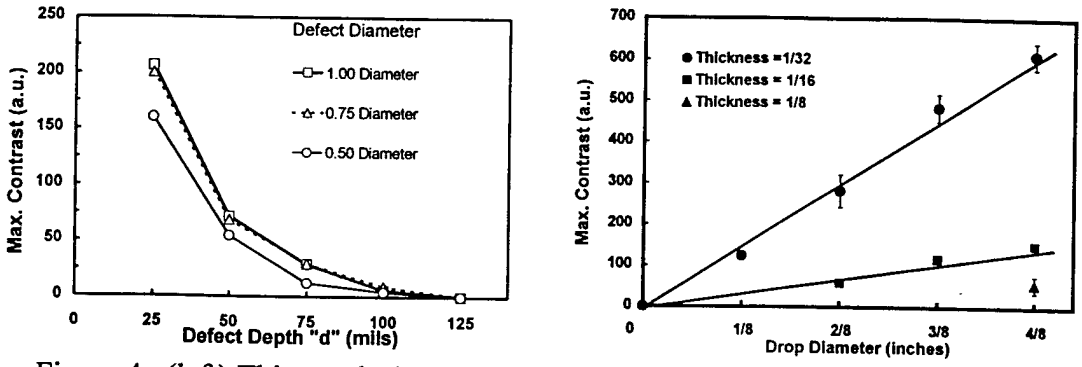

Figure 4. (left) This graph shows the contrast temperature for all flat bottom holes shown on the left of fig. 3 . (right) This graph shows the contrast temperature for all panels with simulated entrapped water shown on the right of figure 3.

the opposite nature of the thermal contrast effects when imaging flat bottom holes compared to when detecting water entrapment. When imaging flat bottom holes it is the thinner region above the defect what ultimately makes this region appear hotter (white region on fig. 3 left). In contrast, it is the excess water acting as a heat sink what makes the region above the entrapped water appear colder (black region on fig. 3 right)

RESULTS AND INTERPRETATION

Figure 4 shows the contrast data of all the samples studied, the graph on the left corresponds to flat bottom hole samples while the graph on the right corresponds to samples with water pockets on the back. From the graph on the left it is clear that the deeper the defect (or the smaller amount of mass loss) the smaller the contrast temperature will be. Also, as the diameter of the defect gets smaller the contrast temperature diminishes. These results have been previously explained[1,2] using a simple lateral heat approximation model. The main result of the model is that the contrast temperature of a sample with a defect can be approximated by

$$\Delta T_{contrast} = \frac{Q}{\rho c}\left(\frac{1}{d}-\frac{1}{t_o}\right)\cdot\left[\frac{R}{2}\frac{t_o}{d(t_o-d)}\right]^{\frac{1}{1-\frac{R}{2}\frac{t_o}{d(t_o-d)}}} \qquad (1)$$

Where the parameters are shown in figure 5 (left) and represent

ΔT_{cont}	contrast temperature
Q	energy deposited on the surface of the sample per unit area
ρc	is the specific heat times the density of the sample
d	distance from surface of the sample to the defect
t_o	is the thickness of the sample
R	is the radius of the defect

This equation correctly accounts for all of the observed experimental results. The term before the square bracket provides the principal contribution to the thermal contrast from which the following can be verified:

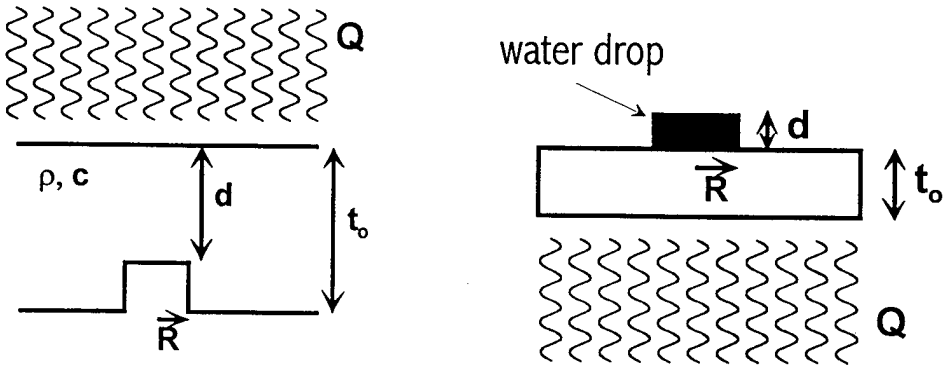

Fig. 5. This figure shows the main parameters used when modeling the thermographic process for mass loss due to corrosion (left) and water entrapment (right)

1. The contrast temperatures (ΔT) increases linearly with the amount of energy deposited per unit area (Q).
2. The higher the specific heat-density of a material ($\rho c \uparrow$) the smaller the contrast temperature becomes ($\Delta T \downarrow$)
3. The closer the defect is to the surface ($d \to 0$) the larger the contrast temperature becomes ($\Delta T \to \infty$)
4. As the defect depth approaches the panel thickness ($d \to t_o$) the contrast temperature vanishes ($\Delta T \to 0$)
5. For a given defect depth d, the thicker the panel ($t_o \to \infty$) the larger the contrast temperature ($\Delta T \uparrow$)

The term in square brackets represent the lateral heat flaw effects and the following can be verified:

6. As defects approach to the surface ($d \to 0$) or as they approach the far end ($d \to t_o$), the lateral heat effects diminish ([lateral factor]$\to$ 1) and the contrast temperature approaches $\Delta T = \frac{Q}{\rho c}\left(\frac{1}{d} - \frac{1}{t_o}\right)$
7. When the defect size decreases ($R \to 0$), the lateral heat factor vanishes ([lateral factor] $\to$ 0) and the thermal contrast disappears ($\Delta T \to 0$)
8. When the defect size increases ($R \to \infty$), then lateral isolation is approached and the lateral heat effects diminish ([lateral factor] $\to$ 1) and the thermal contrast becomes $\Delta T = \frac{Q}{\rho c}\left(\frac{1}{d} - \frac{1}{t_o}\right)$
9. When the thickness of the panel becomes very large ($t_o \to \infty$), the contrast temperature has the limiting value given by $\Delta T = \frac{Q}{\rho c}\frac{1}{d}\left(\frac{R}{2d}\right)^{\frac{1}{1-\frac{R}{2d}}}$

Similar analysis can be conducted for the problem of water entrapment. From the graph on figure 4 (right) it is clear that the thicker the panels are, the smaller the contrast

temperature will be. Also, as the diameter of the defect gets smaller the contrast temperature diminishes. The error bars on the graph represent the effect that different amounts of water had on the thermal contrast. It is obvious from the smallness of the error bars that the effect of the amount of entrapped water on the thermal contrast is minimal. A simple model was previously obtained[3] that used a simple lateral heat approximation. The main result of the model is that the contrast temperature of an sample with water entrapped can be approximated by the following equation if a contact conductivity is used instead of the thermal conductivity, then

$$\Delta T_{peak} = \frac{Q}{\rho c}\frac{d}{r \cdot t_o^2} \cdot \left[\frac{h}{2k}\frac{R}{d} r\right]^{1+\frac{h}{2k}\frac{R}{d} r} \qquad (2)$$

Where the parameters are shown in figure 5 (right) and represent

h	contact conductivity between aluminum and water
k	contact thermal conductivity of aluminum
r	specific heat-density ratio ($r = \rho c/\rho_w c_w$)
d	the height of the water drop
t_o	is the thickness of the aluminum sample
R	is the radius of the water drop

This equation correctly accounts for most of the observed experimental behavior of pulsed thermography as it relates to water entrapment. The terms before the square bracket provide the principal contribution to the thermal contrast from which the following can be verified:

1. The contrast (ΔT) increases linearly with the amount of energy deposited (Q).
2. The higher the specific heat-density of the substrate ($\rho c \uparrow$) the smaller the peak contrast ($\Delta T \downarrow$)
3. As the water content decreases ($d \rightarrow 0$) the contrast vanishes ($\Delta T \rightarrow 0$).
4. As the amount of water grows indefinitely ($d \rightarrow \infty$) the contrast temperature saturates ($\Delta T \rightarrow Q/\rho_1 c_1 t_o$).

CHARACTERIZATION OF CORROSION

There are various types of corrosion present in metallic structures such as pitting, exfoliation, filiform, galvanic and crevice corrosion. Since the first means of corrosion

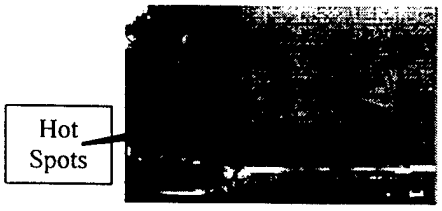

Figure 6. Aluminum lapjoint with three rows of fasteners. There is clear evidence of a hot spots around some fasteners.

protection is by painting the exposed surface or by sealing joined parts, corrosion will always start as hidden. Some of the locations where corrosion can be found are under the paint, around fasteners, inside lap joints, behind panels and on second layers. The ability to detect corrosion thermographically will depend on the amount of contrast generated relative to other contrast generating non-uniformities. Figure 6 shows a thermal image of an aluminum lapjoint with three rows of fasteners. The fasteners appear dark because they are much thicker than the structure being interrogated. Around several of the fasteners there are regions that clearly appear brighter than others as indicated in the figure. These regions can be interpreted as probable corrosion regions, but due to the proximity of the fasteners and the fact that sealant was used, it is difficult to determine if any mass has been lost. At the time of this paper the part could not be cut open in order to make a definite assessment of the defect. In order to make an exact determination of the cause for the hot regions a better knowledge of the part and finite element calculations are needed.

DETECTABILITY REGION

There is a "rule of thumb" that is regularly used to determine the ultimate depth to which a defect of a given size can be detected by thermal methods. This rule states that "those planar defects located at a depth smaller or equal to their cross sectional diameter can be detected thermographically". In light of the simple models presented in this paper, this rule of thumb is not precise. From eq. 1 it can be seen that any planar defect, no matter what its location or cross section is, it will always be possible to detect it thermographically provided that enough energy is deposited on the samples surface. This is direct consequence of the linear dependence of the thermal contrast on the amount of energy deposited on the surface. There is of course the practical limit of not depositing so much energy so as to damage the material.

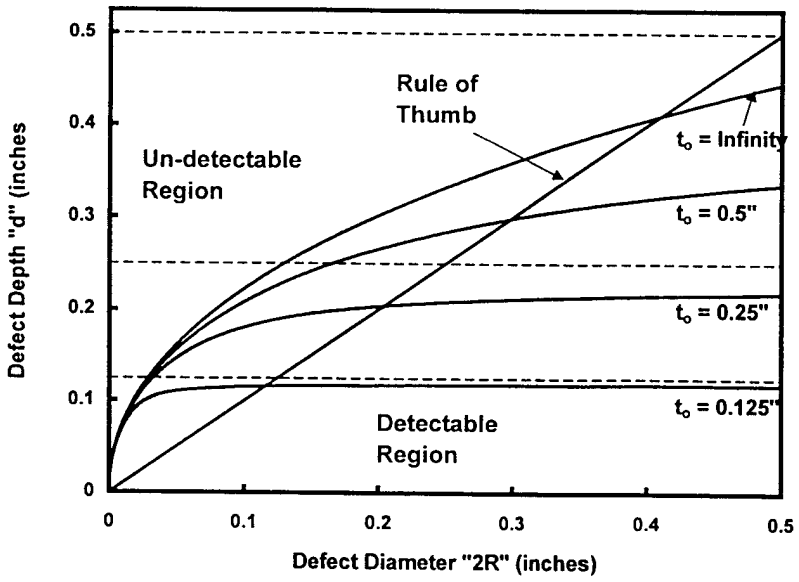

Figure 7. This graph shows curves that separate detectable from undetectable regions of defect of diameter 2R.

More insight can be obtained into this matter by inverting eq. 1 and obtaining a relation between the size of the flaw "2R" and the distance of the flaw from the surface of the sample "d". The following equation is obtained

$$R = 2\frac{d(t_o - d)}{t_o} \cdot \text{finv}\left[\frac{\Delta T_{contrast}\rho c}{Q \cdot \left(\frac{1}{d} - \frac{1}{t_o}\right)}\right] \quad (3)$$

where the function "finv[x]" is the inverse of the transcendental function $y=x^{1/(1-x)}$. Equation 3 can be used to divide the R-d space into "detectable" and "non-detectable" regions. That is, a defect whose radius "R" and location "d" are such that it falls inside the curve defined by equation 3 will be detectable thermographically. If the defect radius and position are such that they fall outside the curve, then for those experimental parameters the defect will be missed. Figure 7 shows boundary curves for various aluminum thickness. Also on that graph is the "rule of thumb" line. Clearly there is a strong discrepancy between the rule of thumb and the previous results.

SUMMARY

We have demonstrated that thermography can detect mass loss and water entrapment. We have presented predictive formulas that can assist the practitioner in determining what type of contrast levels will be obtained for a particular experimental arrangement. We have determined what the depth of resolution is for the detection of mass loss in aluminum 7075T6. When interrogating real structural components, these simple models can only provide approximate answers. For precise determination of the exact nature and extent of the defect a detailed knowledge of the part is required together with more detailed analysis such as finite element models.

ACKNOWLEDGMENT

This work was supported in part by Mr. Bradley Smith of the SERDP program office under document number N0016799WR90311 and by Mr. Jim Kelly of the Office of Naval Research by Work Request under document number N0001498WX20360.

---

1 I. Perez, R. Santos, P. Kulowitch, M. Ryan, "Calorimetric modeling of thermographic data," Proc. of the 1998 SPIE Thermosense XX Conference", Orlando, April 6 - 9, 1998

2 I. Perez, P. Kulowitch, "Modeling of Pulsed Thermography in Anisotropic Media," 25th annual Progress in QNDE, Snowbird, Utah., July 19 - 24, 1998

3 I. Perez, W. R. Davis, P. Kulowitch, "Thermographic modeling of water entrapment," Proc. of the 1999 SPIE, Thermosense XXI Conference, eds. D.H. LeMieux & J.R. Snell, Jr. April 1999, p32-39